the FEBS Journal

Untangling the folding mechanism of the 5_2-knotted protein UCH-L3

Fredrik I. Andersson, David G. Pina, Anna L. Mallam, Georg Blaser and Sophie E. Jackson

University Chemical Laboratory, Cambridge, UK

Keywords
folding kinetics; hyperfluorescent intermediate(s); knotted proteins; protein folding; ubiquitin C-terminal hydrolase

Correspondence
S. Jackson, University Chemical Laboratory, Lensfield Road, Cambridge CB2 1EW, UK
Fax: +44 1223 336362
Tel: +44 1223 762011
E-mail: sej13@cam.ac.uk

(Received 9 December 2008, revised 27 February 2009, accepted 3 March 2009)

doi:10.1111/j.1742-4658.2009.06990.x

Proteins possessing deeply embedded topological knots in their structure add a stimulating new challenge to the already complex protein-folding problem. The most complicated knotted topology observed to date belongs to the human enzyme ubiquitin C-terminal hydrolase UCH-L3, which is an integral part of the ubiquitin–proteasome system. The structure of UCH-L3 contains five distinct crossings of its polypeptide chain, and it adopts a 5_2-knotted topology, making it a fascinating target for folding studies. Here, we provide the first in depth characterization of the stability and folding of UCH-L3. We show that the protein can unfold and refold reversibly *in vitro* without the assistance of molecular chaperones, demonstrating that all the information necessary for the protein to find its knotted native structure is encoded in the amino acid sequence, just as with any other globular protein, and that the protein does not enter into any deep kinetic traps. Under equilibrium conditions, the unfolding of UCH-L3 appears to be two-state, however, multiphasic folding and unfolding kinetics are observed and the data are consistent with a folding pathway in which two hyperfluorescent intermediates are formed. In addition, a very slow phase in the folding kinetics is shown to be limited by proline-isomerization events. Overall, the data suggest that a knotted topology, even in its most complex form, does not necessarily limit folding *in vitro*, however, it does seem to require a complex folding mechanism which includes the formation of several distinct intermediate species.

During the last two decades, an enormous amount of information has been obtained on how proteins fold into their distinctive, 3D structures. Many smaller proteins or protein domains, usually < 100 residues in length, have been thoroughly studied in terms of their folding pathways [1], allowing pieces of the folding puzzle to be solved and mechanisms to be proposed. By contrast, the folding of larger proteins and oligomeric protein complexes has not been investigated to the same extent. There is an even greater dearth of knowledge on the folding mechanisms of polypeptides belonging to the group of proteins possessing deep topological crossings in their polypeptide chains known as 'knots' [2]. These so-called knotted proteins (~ 273 have been discovered to date) have different structures and biological functions, but share an unusual trait in which the polypeptide chain is threaded through a loop formed by a different part of the polypeptide chain to form deep knot-like structures [2,3]. Many of these proteins are found in prokaryotes, for example, the simple trefoil-knotted methyltransferases, YibK and YbeA. Folding studies on these knotted proteins have begun to reveal aspects of the threading and knotting processes that appear to be required for the protein to achieve its active, native structure [4–12]. Recently, however, even more complicated knotted proteins have been discovered in higher eukaryotes such as plants and humans [2,3]. This is

Abbreviation
UCH, ubiquitin C-terminal hydrolase.

highlighted by the 5_2-knotted human ubiquitin C-terminal hydrolase UCH-L3, which contains five topological crossings in its polypeptide chain [3]. UCH-L3 has the most complex topology of any knotted protein discovered to date, and, with the exception of carbonic anhydrase, is the only knotted structure to be identified in humans [3]. The crystal structure of UCH-L3 is shown in Fig. 1A and a schematic representation of the topological crossings of the polypeptide chain shown in Fig. 1B,C.

UCH-L3 is a 26 kDa cysteine protease (pdb code: 1XD3) that belongs to the broader group of ubiquitin C-terminal hydrolases (UCHs). In terms of biological activity, UCH-L3 has been shown to play an important role in the ubiquitin–proteasome system [13,14] and is reported to be active as a monomer [15]. More specifically, UCH-L3 and its structural homologues, such as the human neuronal UCH-L1 [16,17] and yeast Yuh1 [18], proteolytically remove small polypeptide chains linked to the C-terminus of ubiquitin [17,19]. Through this activity, UCHs are thought to control the recycling of ubiquitin and therefore the cellular balance of free ubiquitin [16,17]. Indeed, depletion of these enzymes decreases the overall levels of free ubiquitin in living cells [20]. Recently, certain UCHs have also been assigned an ubiquitin ligase function [15]. In more complex organisms such as humans, many of these enzymes have tissue-specific expression and, as a consequence, might target specific protein substrates; however, very few substrates have been identified to date [13]. Given their tissue-specific expression, it comes as no surprise that impairment of UCH activity has been linked to severe diseases. For example, UCH-L3 has been shown to be upregulated in breast cancer tissues [21], whereas UCH-L1 is associated with neuronal disorders such as Parkinson's disease [22–24].

No stability or folding studies on any of the 5_2-knotted UCH proteins have been reported, nor has a function for their knotted structure been elucidated. However, it has been suggested that the knot in UCH-L3 might make the protein more resistant to unfolding and thereby minimize the risk of degradation by the 26*S* proteasome [3,25].

Given the current lack of knowledge regarding both the stability and folding of the 5_2-knotted ubiquitin hydrolases, we set out to perform an in-depth stability and folding study on UCH-L3. We examined the unfolding of UCH-L3 under equilibrium conditions using chemical denaturants and both fluorescence and far-UV CD as probes of tertiary and secondary structure, respectively. Despite its knotted topology, UCH-L3 unfolds reversibly *in vitro* without the need for molecular chaperones. A kinetic study of both unfolding and refolding reactions revealed complex kinetics in which several unfolding and refolding phases were observed. The data are consistent with a folding mechanism in which two hyperfluorescent intermediates are populated. The results are compared with our previous study on the folding pathways of the 3_1-knotted methyltransferases YibK and YbeA.

Results

Chemical denaturation of UCH-L3 is fully reversible *in vitro*

Pure recombinant UCH-L3 was produced by overexpression in *Escherichia coli* and purified to homogeneity via sequential chromatography. The protein was shown to be pure using both SDS/PAGE and MS analysis. One common strategy for probing the tertiary structure of proteins is to measure the intrinsic fluorescence from aromatic residues such as tyrosine and

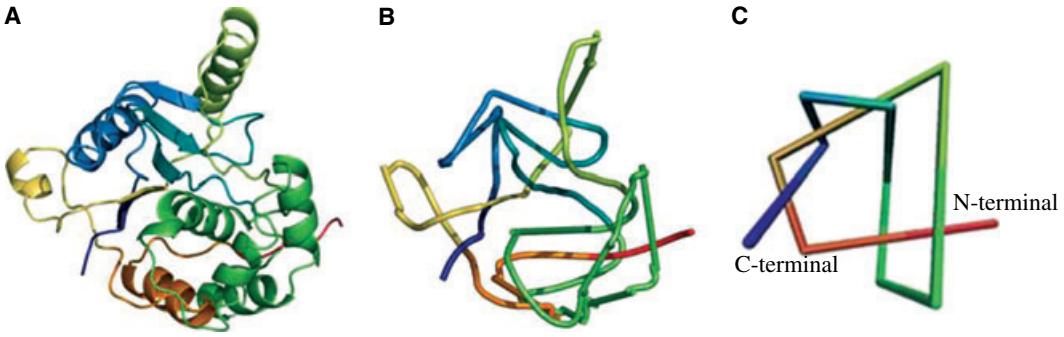

Fig. 1. Structure of UCH-L3. Crystal structure of UCH-L3 (A). Representation of the 5_2-crossings are depicted in (B) and (C). (C) is adapted from Virnau *et al.* [3].

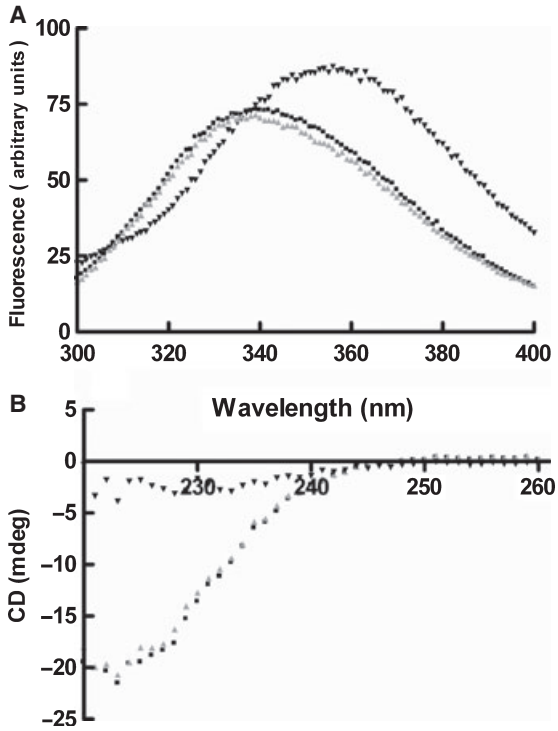

Fig. 2. Reversibility of UCH-L3 unfolding in urea. (A) Fluorescence spectra for native (■), denatured (▼) and renatured (▲) UCH-L3. (B) Far-UV CD-spectra for native (■), denatured (▼) and renatured (▲) UCH-L3.

tryptophan. The fluorescence spectrum of native UCH-L3 shows a λ_{max} at 340 nm (Fig. 2A). Upon incubation of the protein at high urea concentrations, there is a slight increase in fluorescence intensity and a red-shift of λ_{max} to 358 nm, consistent with unfolding (Fig. 2A). To establish that the change in fluorescence observed was caused by a global unfolding event, and not local unfolding in the vicinity of the two tryptophan residues (Trp6 and Trp29), the effects of urea on the secondary structure of UCH-L3 were also examined using far-UV CD. The typical negative ellipticity at 222 nm, caused by the α helices in the structure and observed for native UCH-L3, was absent for the sample incubated in 7 M urea (Fig. 2B).

Tests of the reversibility of unfolding of UCH-L3 were also undertaken. A denatured sample of UCH-L3 in high concentrations of urea was diluted sufficiently to allow refolding, which was monitored using fluorescence and far-UV CD spectroscopy. Denaturation of UCH-L3 proved to be fully reversible under the conditions used; the spectra of a sample of native UCH-L3 that had never been unfolded and one of a sample that had been unfolded then refolded were superimposable (Fig. 2A,B).

Equilibrium unfolding of UCH-L3 follows a two-state model

To gain insight into the conformational stability of UCH-L3, unfolding curves were measured under equilibrium conditions with urea as the chemical denaturant. The degree of unfolding was measured using tryptophan fluorescence and far-UV CD (Fig. 3A,B). Equilibrium data from both experiments were fit separately to a two-state model [26] to calculate: $[D]_{50\%}$, the midpoint of the unfolding transition;$\Delta G^{H_2O}_{D-N}$, the difference in free energy between the native and denatured states in the absence of denaturant; and m_{D-N}, a measure of the change in solvent-accessible surface area between the native and denatured states; these values were approximately −3 M, 7 kcal·mol^{-1} and 2.4 kcal·mol^{-1}·M^{-1}, respectively (Table 1). Interestingly, a small but consistent discrepancy (∼ 7%) between the values of $[D]_{50\%}$ obtained from the fluorescence and

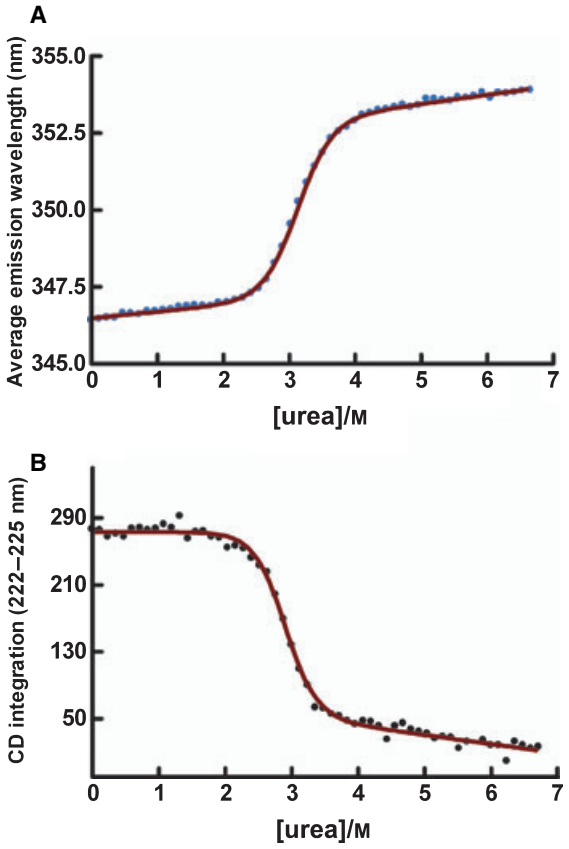

Fig. 3. Equilibrium urea denaturation curves from (A) fluorescence data: the average emission wavelength calculated from the spectra between 300 and 400 nm (●); (B) far-UV CD data obtained by integration of the CD-signal between 222 and 225 nm (●). The red lines display the best fit of the data to a two-state model.

Table 1. Thermodynamic parameters for the denaturation of UCH-L3 by urea. The parameters are from the best fit of the data to a two-state model (Eqn 3) using KALEIDAGRAPH 4. Values for $\Delta G^{H_2O}_{D-N}$ were calculated using Eqn (4).

Thermodynamic parameters	Far-UV CD	Fluorescence
m_{D-N} (kcal·mol^{-1}·M^{-1})	2.5 ± 0.2	2.28 ± 0.06
$\Delta G^{H_2O}_{D-N}$ (kcal·mol^{-1})	7.3 ± 0.4	7.11 ± 0.2
$[D]_{50\%}$ (M)	2.9 ± 0.02	3.12 ± 0.01

far-UV CD data was observed (Table 1). Although the values of $[D]_{50\%}$ obtained using the different probes are not quite within error, the behaviour of UCH-L3 is most consistent with a two-state model of folding under equilibrium conditions.

UCH-L3 folds via a hyperfluorescent state

Having established that the unfolding of UCH-L3 in urea under equilibrium conditions was fully reversible, a study of the unfolding and folding kinetics was undertaken. Tryptophan fluorescence was used as a sensitive probe of the state of the protein.

Unfolding kinetics

First, stopped-flow techniques were used to rapidly mix native UCH-L3 and buffer containing high concentrations of urea, and unfolding traces were collected. The unfolding data were a good fit to a first-order process described by a single exponential plus drift (Eqn 1) (Fig. 4A). The logarithm of the unfolding rate constant obtained from these fits is shown as a function of urea concentration in Fig. 5.

Refolding kinetics

Subsequently, refolding of UCH-L3 was initiated by injecting denatured UCH-L3 (in 8 M urea) into buffer containing lower concentrations of denaturant. The expected loss of fluorescence upon refolding was first observed in stopped-flow experiments over a time scale of 10–500 s. The refolding traces were a good fit to an equation describing a double-exponential process (Eqn 2), resulting in two rate-constants k_1 and k_2 (Fig. 4B). In order to obtain accurate rate constants for the slowest folding phase (phase 2), longer traces were collected by using manual-mixing experiments on a fluorimeter. The dependence of the rate constants for these two phases on the urea concentration is shown in Fig. 5. It is clear from the chevron plot shown that k_1 is the folding phase corresponding to the unfolding phase observed in the single-jump unfolding experiment (Fig. 5).

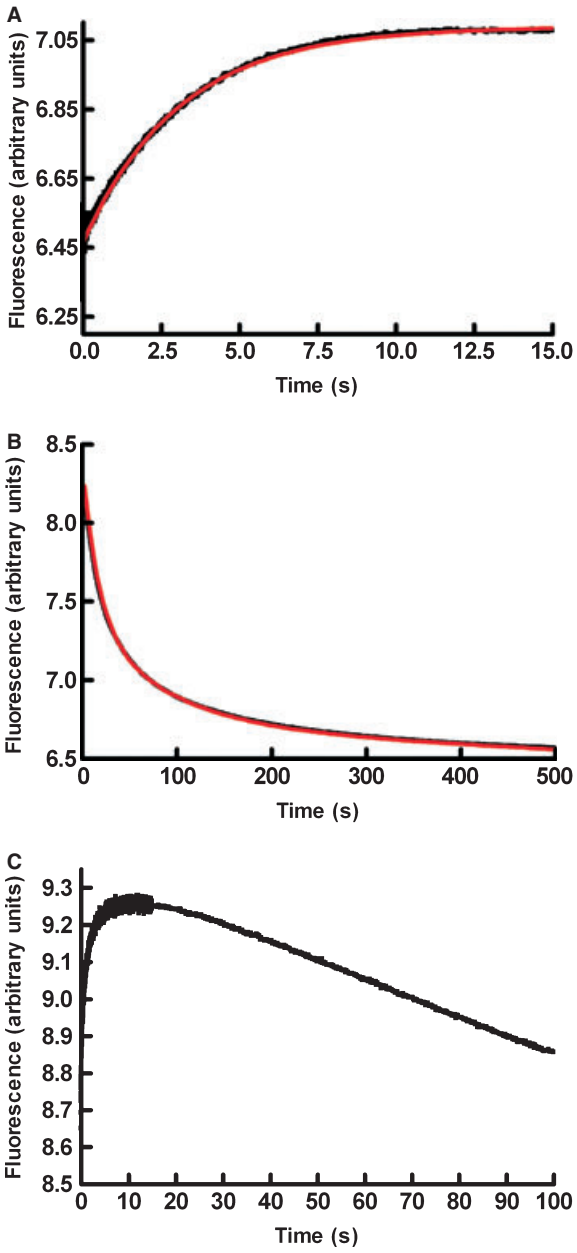

Fig. 4. UCH-L3 kinetic folding and unfolding traces. (A) UCH-L3 (2 μM) unfolding trace measured at 4.9 M urea at 25 °C using stopped-flow techniques. The red line displays the best fit of the data to a single exponential process. (B) UCH-L3 (2 μM) refolding traces at 0.9 M urea at 25 °C using stopped-flow techniques. The red line shows the best fit of the data to a double-exponential process. (C) Refolding traces recorded over shorter time scales in 2 M urea at 25 °C, highlighting the formation of the hyperfluorescent state.

Although the signal expected for the refolding of UCH-L3 was observed in the experiments described

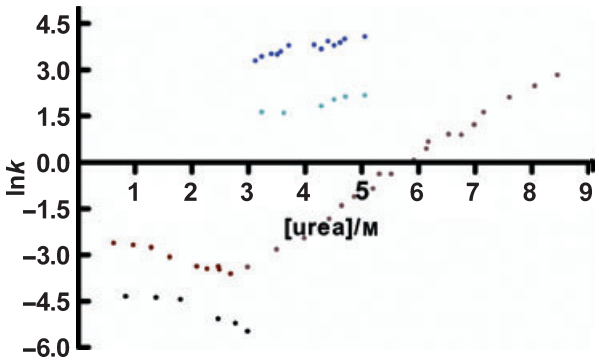

Fig. 5. Chevron plot for the unfolding and folding kinetics of UCH-L3. Depicted are the rate constants for the only observed unfolding phase in the single-jump experiments (●), the two slow refolding phases: k_1 (●) and k_2 (●), and the unfolding rate constants $k_{HyF\_unfold\_1}$ (●) and $k_{HyF\_unfold\_2}$ (●) corresponding to the unfolding of the hyperfluorescent intermediates.

above, when refolding was analysed over shorter time scales, faster phases (between 0.4 and 30 s) were also seen in which the signal corresponded to an increase in fluorescence. These phases occurred prior to the slower biphasic decrease in fluorescence (Fig. 4C). Unfortunately, these fast refolding phases were extremely problematic to fit, either individually or globally, and rate constants could not be obtained to a satisfactory degree of accuracy (because there are multiple phases that are not well separated). However, the fast phases leading up to the hyperfluorescent state were seen to depend upon the urea concentration (data not shown). These data are consistent with the formation of hyperfluorescent intermediates during the folding of UCH-L3.

Interrupted refolding experiments reveal two additional unfolding phases corresponding to unfolding of the hyperfluorescent states

The fast folding phases associated with formation of the hyperfluorescent intermediates were extremely difficult to analyse adequately. Therefore, an alternative approach was chosen to try to detect the corresponding unfolding phases of the intermediates using interrupted refolding assays. In these experiments, denatured UCH-L3 was first refolded for a certain delay time, sufficient to populate the hyperfluorescent intermediate states but insufficient to form the native state, unfolding was then initiated and unfolding traces collected. At delay times between 1 and 7 s, unfolding phases resulting in a decrease in fluorescence were detected (Fig. 6A). These rapid unfolding phases were well described by a double-exponential process giving rise to the two unfolding rate constants ($k_{HyF\_unfold\_1}$ and $k_{HyF\_unfold\_2}$) (Fig. 5). These findings support the previous suggestion that at least two hyperfluorescent intermediates (HyF-I_1 and HyF-I_2) are formed during the refolding of UCH-L3.

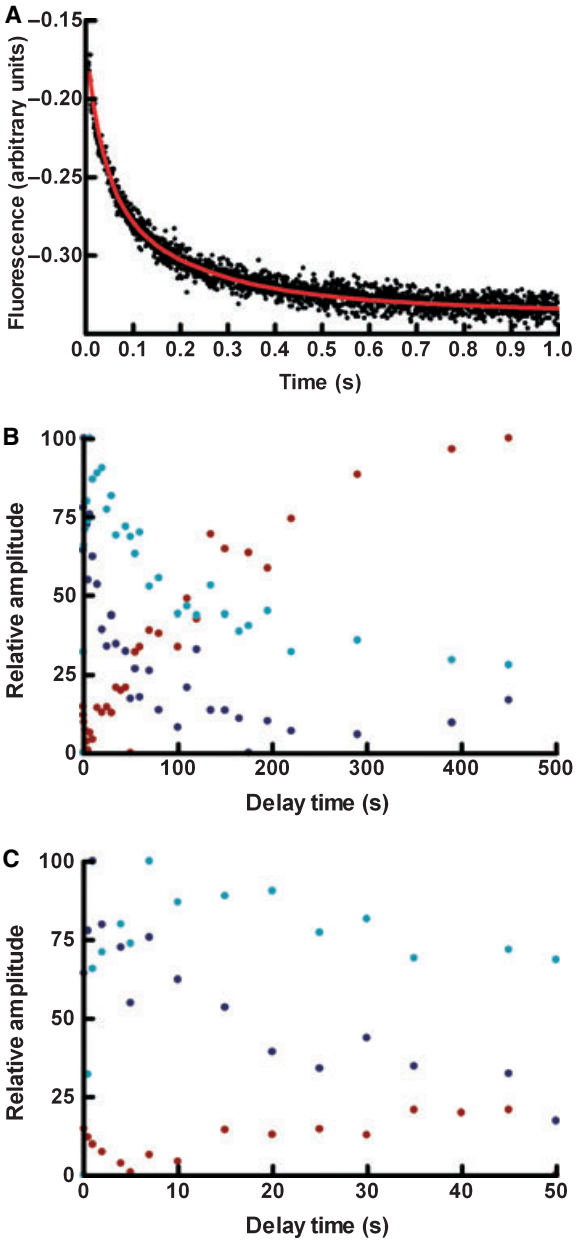

Fig. 6. Interrupted refolding experiments probe the unfolding phases corresponding to the hyperfluorescent intermediate states. (A) Unfolding trace of UCH-L3 (5 μM) at 25 °C and 4.7 M urea, observed after 7 s of refolding. The red line displays the best fit of the data to a double-exponential process. (B) The amplitude change for the major folding phase observed in single-jump experiments (●), and hyperfluorescent intermediates HyF-I_1 (●) and HyF-I_2 (●). (C) A magnified picture of the amplitude plot shown in (B) over short time scales.

Hyperfluorescent state: the two hyperfluorescent intermediate states are populated rapidly during refolding

In order to gain further insights into the nature of HyF-I_1 and HyF-I_2, the time-dependent formation of the different species along the UCH-L3 folding pathway was studied using interrupted refolding experiments with varying delay times. This method assumes that after various delay times the amplitude of the unfolding phase(s) are proportional to the number of molecules in that state on the folding pathway [27]. Consequently, denatured UCH-L3 was refolded into 0.9 M urea for various delay times and then jumped back into unfolding conditions (4.7 M urea), thus allowing the time evolution and formation of the various intermediate states to be monitored. The two hyperfluorescent intermediates were populated quickly, with formation of HyF-I_2 (light blue phase) being slightly slower than that of HyF-I_1 (dark blue) (Fig. 6B,C). As expected, at longer delay times (400 s), the amplitudes associated with the different intermediate states diminished to zero as the intermediate converted to the native state. Moreover, the rate constants for their decay were very similar (HyF-I_1: 0.024 s^{-1} and HyF-I_2: 0.02 s^{-1}). By contrast, the population of the species corresponding to the major folding event (red phase) observed in single-jump experiments, displayed a significant lag in its formation and was only observed after delay times of 40–50 s, reaching a maximum after 300–400 s (Fig. 6B,C). The rate constant for the formation of the species associated with this phase is 0.045 s^{-1}, which is in good agreement with the k_1 folding rate constant at 0.9 M urea (Fig. 5). These results were consistent with our proposed model and indicative of the population of the hyperfluorescent intermediates decaying as the population of the native state species increased.

The folding pathway of UCH-L3 is limited by proline isomerization

In the native states of proteins, prolyl peptide bonds are usually in a fixed *cis* or *trans* conformation. However, when a protein is unfolded, the structure which constrained the prolyl bond into a specific conformation is lost and an equilibrium between *cis* and *trans* conformations is established, in which the *trans* state is favoured over *cis* at a ratio of $\sim 4:1$ [28]. Upon refolding, isomerization of these peptidyl–prolyl bonds back to their native conformation can be rate limiting because this process is usually slow, with a rate constant of around 0.04–0.08 s^{-1} [28]. Because UCH-L3 has 12 proline residues, one of which is in a *cis* conformation in the native state (Pro48), it is highly probable that the slow refolding phase (the black phase, giving rise to k_2) is caused by a rate-limiting proline isomerization reaction. In order to investigate this further, interrupted unfolding experiments using stopped-flow techniques were undertaken. In these experiments, UCH-L3 was first unfolded for various delay times (1–400 s) at high concentrations of guanidine hydochloride (under these conditions the unfolding rate constant is very fast, ~ 400 s^{-1}). Subsequent refolding was then initiated by diluting the sample in buffer containing a low concentration of denaturant. At the shortest unfolding delay times, no peptidyl–prolyl bond isomerization can occur, resulting in a native-like conformation for all proline residues [27]. The kinetic refolding traces (Fig. 7A) obtained from these experiments with different delay times were fit globally to a double-exponential equation with shared values for the two rate constants, k_1 and k_2.

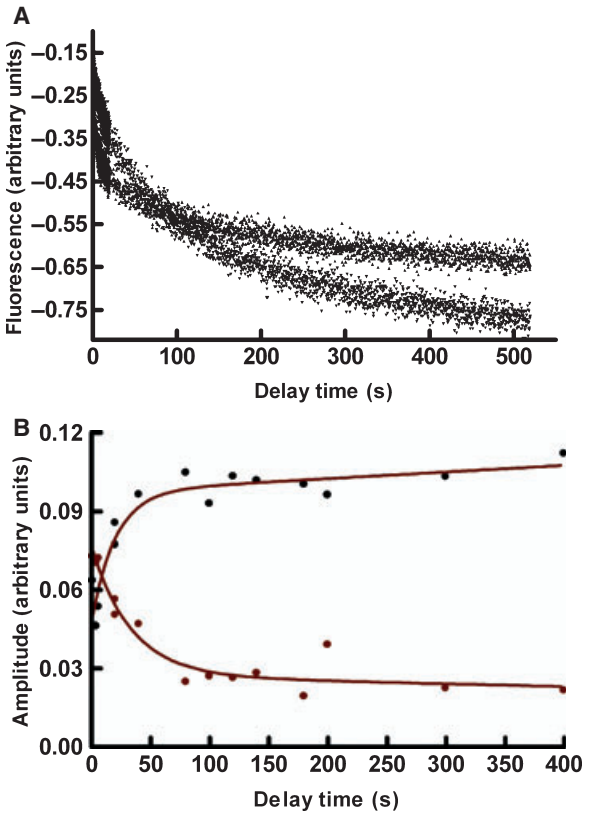

Fig. 7. Interrupted unfolding experiments. (A) Refolding traces of UCH-L3 (2 μM) at 25 °C in 0.93 M guanidine hydrochloride that had been unfolded in high concentrations of guanidine hydrochloride for 1 s (▲) or 30 min (▼). (B) Plot of the amplitude change for k_1 (●) and k_2 (●) with respect to unfolding time. The red lines display the best fit of the data to a single exponential process.

A plot of the amplitudes obtained from interrupted unfolding experiments is a direct measure of the population of molecules that give rise to a particular kinetic phase [27]. With increasing unfolding delay times, an increase in molecules folding with a rate constant of k_2 (black phase) was observed. The rate constant with which this phase developed is 0.04 s^{-1}. Such behaviour is consistent with slow proline isomerization processes occurring in the denatured state, showing that the slowest phase observed in the refolding of UCH-L3 is limited by a proline isomerization event. By contrast, a decrease in amplitude was observed for the faster of the two slow refolding phases (the red phase, corresponding to k_1) with increasing delay times, with a similar rate constant to that observed for the development of the slowest refolding phases (black phase) (Fig. 7B). The overall change in amplitude for the sum of the two phases did not vary with unfolding delay time, indicating that even at the shortest delay times, UCH-L3 was fully unfolded (data not shown).

Discussion

In this study, we investigated the stability and folding of the 5_2-knotted ubiquitin hydrolase UCH-L3. UCH-L3 is an essential enzyme present in various tissues in the human body, where it functions as a deubiquitinating enzyme, hydrolysing C-terminal ubiquityl esters [13,17]. Through this activity, UCH-L3 and other ubiquitin hydrolases control the level of free monoubiquitin in the cell and hence play a vital role in several processes, including the ubiquitin–proteasome pathway [13].

The chemical denaturant urea was used to reversibly unfold UCH-L3, enabling us to characterize the stability and folding/unfolding kinetics of the protein *in vitro*. Using tryptophan fluorescence as a probe of tertiary structure, a red-shift was observed upon chemical denaturation, consistent with a process in which buried or partially buried tryptophan residues become exposed to the solvent and the aqueous environment [29]. In addition, unfolding was measured using far-UV CD as a probe of secondary structure, and the urea-denatured state was shown to have no stable residual secondary structure. Both fluorescence and far-UV CD were used to establish that the unfolding of UCH-L3 was fully reversibly under the conditions used. These results show that, despite its complex knotted topology, UCH-L3 is able to refold spontaneously *in vitro* without the need for molecular chaperones. These findings agree well with what has been reported for the smaller and simpler trefoil knotted proteins YibK and YbeA [4,5,7].

Under equilibrium conditions, the unfolding of UCH-L3 appears to follow a simple two-state folding model, in which only native and denatured states are significantly populated. This type of behaviour is common for smaller proteins [26]. If a protein is a true two-state folder under equilibrium conditions, then the thermodynamic parameters obtained by fitting the data from different structural probes should be the same [30]. For UCH-L3, the thermodynamic parameters m_{D-N} and $\Delta G^{H_2O}_{D-N}$, obtained from the fits of fluorescence and the far-UV CD data, are within error, suggesting that it is a two-state system (Table 1). However, the thermodynamic parameter $[D]_{50\%}$ varies slightly between the two data sets (Table 1), indicating that an intermediate might be populated under equilibrium conditions, albeit at very low levels. Although some proteins have folding intermediates that are stable enough with respect to the denatured state to be sufficiently populated and observable under equilibrium conditions [31], many proteins which show apparent two-state behaviour under equilibrium conditions have complex kinetics with several folding and/or unfolding phases resulting from the formation of folding intermediates [32].

Thorough kinetic analysis of the folding and unfolding of UCH-L3 revealed several phases which were investigated using a series of single- and double-jump experiments. First, UCH-L3 refolding was shown to be limited by proline isomerization events. The rate at which this process occurs ($\sim$ 0.04 s^{-1}) agrees well with that observed for other proteins, for example RNase A and ANG, limited by proline isomerization events [33]. Second, single-jump refolding experiments on UCH-L3 showed that two hyperfluorescent intermediates were rapidly populated upon refolding from the denatured state, as seen by the initial increase in the fluorescence signal (Fig. 4C). Such behaviour has not been reported for the trefoil-knotted methyl transferases [5,7]. However, we were unable to determine accurate folding rate constants for the formation of these hyperfluorescent intermediates despite using several different fitting strategies. A likely cause of these difficulties is that the refolding phases are overlapping. Instead, we chose to characterize their corresponding unfolding phases by performing interrupted refolding double-jump assays [27]. In these assays, denatured UCH-L3 was refolded for various times to populate the hyperfluorescent states and then subjected to unfolding at high urea concentrations. Using this strategy, two additional unfolding phases (rate constants $k_{HyF\_unfold\_1}$ and $k_{HyF\_unfold\_2}$) were obtained. These data strongly suggest that there are two hyperfluorescent intermediates, HyF-I_1 and HyF-I_2, on the folding pathway of UCH-L3.

Kinetic intermediates which are hyperfluorescent have also been observed for several other proteins [34–37]. Judging from the amplitude plot for the interrupted refolding experiments (Fig. 6B,C), it appears that the hyperfluorescent intermediates are populated rapidly (1–10 s), these then convert to the native state over a longer time scale. That HyF-I_1 failed to decay as HyF-I_2 is populated, suggests that they are formed in parallel. Such parallel pathways can arise from a heterogeneous denatured state. Indeed, such a mechanism has recently been proposed for the knotted protein YibK [8]. Based on our results, and comparisons with other knotted proteins, we propose a kinetic scheme for the folding of UCH-L3 (Fig. 8). In this case, we propose that the intermediate states HyF-I_1 and HyF-I_2 are on-pathway, as reported for other knotted proteins [5].

The origin of the hyperfluorescence of the folding intermediates is not investigated in detail in this study and extensive additional site-directed mutagenesis studies on residues in close proximity to Trp6 and Trp29 would be needed to examine this comprehensively. However, by visual inspection of the crystal structure, an educated guess can be made. In the denatured state, tryptophan residues are quenched by the solvent giving rise to a rather low fluorescence signal. In the hyperfluorescent state populated during refolding, quenching may well be diminished by a reduction in solvent interactions and partial burial of the side chains of the tryptophan residues in a hydrophobic environment. Such a hydrophobic environment may be formed by the hydrophobic collapse of the polypeptide chain in this region (both tryptophan residues are located near the N-terminus of the protein). If HyF-I_1/HyF-I_2 are on-pathway intermediates, it is likely that the hydrophobic environment is created by interactions similar to those present in the native state. Such hydrophobic contacts could be provided by Lys110, Met111, Leu227 and Ala229, which are < 5 Å from indole ring of Trp29 in the native structure (Fig. S1) [14,18]. The subsequent quenching of fluorescence in the native state may arise from further structural rearrangements in this region of the protein upon further folding.

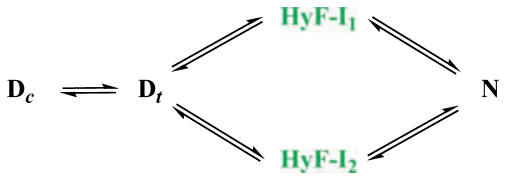

Fig. 8. Proposed kinetic scheme for the folding of UCH-L3. Schematic representation of the possible folding pathway obtained from all experimental kinetic data.

These might include repositioning of residue Cys50, which has been shown to be located orthogonally 3 Å from the indole ring of Trp29 [18] (Fig. S1), and which could therefore participate in an excited state proton-transfer reaction [38], thereby quenching the fluorescence. Indeed, polar side chains are known to quench tryptophan fluorescence [38]. This has been reported for the well-studied Im7 protein that folds via an on-pathway hyperfluorescent intermediate. In this case, the quenching of Trp75 in the native state is achieved by close contact with a neighbouring histidine side chain [34,39].

To summarize, we present here the first characterization of the stability and folding of the human 5_2-knotted protein ubiquitin hydrolase, UCH-L3. The protein has one of the most complex knotted topologies observed to date [3]. Despite its complex structure, with five distinct crossings of the polypeptide chain, UCH-L3 unfolds reversibly *in vitro* without the need for molecular chaperones. Moreover, the folding kinetics reveal a complex folding mechanism which includes the formation of two hyperfluorescent intermediate states. This initial study now paves the way for more detailed kinetic studies of the folding pathways of these structurally tangled proteins.

Experimental procedures

Plasmids and materials

The plasmid pRSET/UCH-L3 was a kind gift from the laboratory of H. Ploegh (Whitehead Institute for Biomedical Research, Cambridge, MA, USA). Pre-cast SDS/PAGE gels and Coomassie Brilliant Blue stain were from Invitrogen (Carlsbad, CA, USA) and all chromatography material was purchased from GE Healthcare (Piscataway, NJ, USA). All other chemicals were analytical grade and purchased from Sigma-Aldrich (St Louis, MO, USA) or Melford Laboratories (Chelsworth, UK).

Protein expression, purification and quantification

Human UCH-L3 was purified as described previously [17], however an additional mono-Q ion-exchange step was used to improve purity. Purified UCH-L3 was aliquoted and flash-frozen in buffer A (50 mM Tris, pH 7.6, 0.5 mM EDTA, 5 mM dithiothreitol) and stored at −80 °C. Purified UCH-L3 was subjected to MS analysis to confirm size and identity and SDS/PAGE to judge purity. The concentration of UCH-L3 monomers was determined spectrophotometrically using an extinction coefficient at 280 nm of 20 065 $M^{-1} \cdot cm^{-1}$. Care was taken that the reference buffer also contained exactly the same amount of dithiothreitol as

the protein sample, because dithiothreitol can contribute to absorbance at 280 nm.

Spectroscopic measurements

Fluorescence measurements were made using a 1 cm path-length cuvette in a Cary Eclipse fluorimeter (Varian, Palo Alto, CA, USA). An excitation wavelength of 280 nm was used, with a band pass of 5 nm for excitation and 10 nm for emission. Emission spectra were recorded between 300 and 400 nm at a scan rate of 1 nm·s^{-1}.

Equilibrium unfolding experiments

All equilibrium measurements were performed at 25 °C in buffer A. For the unfolding curves a stock of urea (~ 8 M in buffer A) was prepared volumetrically and stored at −20 °C until use. The exact concentration of urea was determined from its refractive index using an Atago 1T refractometer (Bellingham & Stanley Ltd., Tunbridge Wells, UK). The urea stock was then diluted with buffer A, such that a concentration range of 0–7 M was obtained in 800 μL aliquots. This procedure was performed using a Hamilton Microlab apparatus (Taylor Scientific, St Louis, MO, USA). For unfolding curves, 100 μL of UCH-L3 in buffer A was added to the 800 μL aliquots of the various urea concentrations to yield a final concentration of protein of 3 μM. The protein/denaturant mixtures were then left to equilibrate for 3–20 h at room temperature after which no change in spectroscopic signal was observed. Unfolding was followed by Trp fluorescence by measuring the area under the curves (from 300 to 400 nm) as described elsewhere [40]. Far-UV CD spectra were acquired using an Applied Photophysics chirascan spectrometer (Leatherhead, UK) and the CD signal integrated between 222 and 225 nm.

Reversibility tests

The reversibility of the unfolding of UCH-L3 was examined both by fluorescence (Cary eclipse Fluorimeter; Varian, Palo Alto, CA, USA) and far-UV CD (Applied Photophysics chirascan spectrometer). UCH-L3 was diluted to a final concentration of 2 μM in either buffer A or 8 M urea containing buffer A. The samples were then incubated for 1 h at 25 °C and the denatured sample was allowed to refold by dilution of the sample with buffer A (such that the final concentration of urea in both cases was 0.65 M urea). The renaturation reaction was left for 1–5 h before spectra were acquired.

Unfolding and refolding kinetics

The unfolding and refolding kinetics of UCH-L3 were measured using stopped-flow techniques (for shorter time scales) or by manual mixing (for longer time scales) using an Applied Photophysics stopped-flow spectrometer or a Cary Eclipse fluorimeter, respectively. Native or denatured UCH-L3 (22 μM) was prepared in buffer A or buffer A plus urea as appropriate. Native or denatured UCH-L3 protein was then rapidly diluted 1 : 10 in buffer A or buffer A containing urea, resulting in a final protein concentration of 2 μM, with various concentrations of urea. The exact urea concentration was determined as described above. A cut-off filter of 320 nm was employed in the stopped-flow apparatus, whereas an emission wavelength of 360 nm was used for the traces collected by manual mixing in the Cary Eclipse fluorimeter.

Interrupted unfolding experiments

Native UCH-L3 (72 μM) was unfolded for various delay times (1–300 s) by mixing 1 : 36 in ~ 5.6 M guanidine hydochloride. After a specific delay time, refolding was initiated by rapid mixing and dilution into buffer A, such that the final guanidine hydochloride concentration and protein concentrations were 0.93 M and 2 μM respectively. Trp fluorescence was monitored and data acquired using the stopped-flow apparatus and settings described above.

Interrupted refolding experiments

Denatured UCH-L3 in 5.5 M urea was refolded for various delay times (0.1–500 s) by mixing 1 : 5 in buffer A, such that the concentration of urea was 0.93 M. Unfolding was then initiated by rapid dilution into high concentrations of urea, such that the final urea concentrations varied between 4 and 6 M. The final concentration of protein after the two mixing and dilution steps was 5 μM. The double-jump experiments were preformed on a stopped-flow instrument as described above.

Data analysis

The kinetic parameters, including the rate constants for the different phases were obtained from fitting the fluorescence traces to various equations (see below) using either KALEIDAGRAPH 4 or GRAPHPAD PRISM. Normally, the unfolding traces were fit to a single exponential process or a single exponential with a drift (Eqn 1), where A_1 is the amplitude, k_1 is the rate constant, n is the drift of the signal and C is the offset.

$$y = A_1(1 - \exp(-k_1 t)) + nt + C \quad (1)$$

The refolding and unfolding traces from the interrupted refolding assays fit well to a process described by a double exponential with drift (Eqn 2), where A_1 is the amplitude of phase 1, k_1 is the rate constant for phase 1, A_2 is the ampli-

tude of phase 2, k_2 is the rate constant for phase 2, n is the drift of the signal and C is the offset.

$$y = A_1(1 - \exp(-k_1 t)) + A_2(1 - \exp(-k_2 t)) + nt + C \quad (2)$$

To measure the changes in amplitude in the double-jump assays, traces were fit globally with shared rate constants.

The equilibrium values for $[D]_{50\%}$ and m_{D-N} were calculated using Eqn (3), where α_N and α_D are the spectroscopic signals of the native and denatured states in the absence of denaturant and β_N and β_D are the slopes of the native and denatured baselines and $[D]$ is the concentration of denaturant.

$$F = \frac{(\alpha_N + \beta_N[D]) + ((\alpha_D + \beta_D[D])\exp((m_{D-N}([D] - [D]_{50\%})))/RT}{1 + \exp(m_{D-N}([D] - [D]_{50\%}))/RT} \quad (3)$$

The value for $\Delta G^{H_2O}_{D-N}$was then calculated using Eqn (4).

$$\Delta G^{H_2O}_{D-N} = m_{D-N}[D]_{50\%} \quad (4)$$

Acknowledgements

This study was supported by the Leverhulme Trust. The authors are grateful to Dr Chittaranjan Das (Purdue University, West Lafayette, IN, USA) for purified UCH-L3 as a control protein for stopped-flow refolding experiments to verify the presence of the hyperfluorescent state.

References

1 Mallam AL & Jackson SE (2008) Use of protein engineering techniques to elucidate protein folding pathways. *Prog Nucleic Acid Res Mol Biol* **84**, 57–114.
2 Taylor WR (2007) Protein knots and fold complexity: some new twists. *Comput Biol Chem* **31**, 151–162.
3 Virnau P, Mirny LA & Kardar M (2006) Intricate knots in proteins: function and evolution. *PLoS Comput Biol* **2**, 1074–1079.
4 Mallam AL & Jackson SE (2005) Folding studies on a knotted protein. *J Mol Biol* **346**, 1409–1421.
5 Mallam AL & Jackson SE (2006) Probing nature's knots: the folding pathway of a knotted homodimeric protein. *J Mol Biol* **359**, 1420–1436.
6 Mallam AL & Jackson SE (2007) The dimerization of an [alpha]/[beta]-knotted protein is essential for structure and function. *Structure* **15**, 111–122.
7 Mallam AL & Jackson SE (2007) A comparison of the folding of two knotted proteins: YbeA and YibK. *J Mol Biol* **366**, 650–665.
8 Mallam AL, Morris ER & Jackson SE (2008) Exploring knotting mechanisms in protein folding. *Proc Natl Acad Sci USA* **105**, 18740–18745.
9 Mallam AL, Onuoha SC, Grossmann JG & Jackson SE (2008) Knotted fusion proteins reveal unexpected possibilities in protein folding. *Mol Cell* **30**, 642–648.
10 Sulkowska JI, Sulkowski P, Szymczak P & Cieplak M (2008) Tightening of knots in proteins. *Phys Rev Lett* **100**, doi:10.1103/PhysRevLett.100.058106.
11 Wallin S, Zeldovich KB & Shakhnovich EI (2007) The folding mechanics of a knotted protein. *J Mol Biol* **368**, 884–893.
12 Mallam AL (2009) How does a knotted protein fold? *FEBS J* **276**, 365–375.
13 Love KR, Catic A, Schlieker C & Ploegh HL (2007) Mechanisms, biology and inhibitors of deubiquitinating enzymes. *Nat Chem Biol* **3**, 697–705.
14 Misaghi S, Galardy PJ, Meester WJN, Ovaa H, Ploegh HL & Gaudet R (2005) Structure of the ubiquitin hydrolase UCH-L3 complexed with a suicide substrate. *J Biol Chem* **280**, 1512–1520.
15 Liu YC, Fallon L, Lashuel HA, Liu ZH & Lansbury PT (2002) The *UCH-L1* gene encodes two opposing enzymatic activities that affect alpha-synuclein degradation and Parkinson's disease susceptibility. *Cell* **111**, 209–218.
16 Larsen CN, Krantz BA & Wilkinson KD (1998) Substrate specificity of deubiquitinating enzymes: ubiquitin C-terminal hydrolases. *Biochemistry* **37**, 3358–3368.
17 Larsen CN, Price JS & Wilkinson KD (1996) Substrate binding and catalysis by ubiquitin C-terminal hydrolases: identification of two active site residues. *Biochemistry* **35**, 6735–6744.
18 Johnston SC, Riddle SM, Cohen RE & Hill CP (1999) Structural basis for the specificity of ubiquitin C-terminal hydrolases. *EMBO J* **18**, 3877–3887.
19 Pickart CM & Rose IA (1985) Ubiqutin carboxyl-terminal hydrolase acts on ubiqutin carboxyl-terminal amides. *J Biol Chem* **260**, 7903–7910.
20 Walters BJ, Campbell SL, Chen PC, Taylor AP, Schroeder DG, Dobrunz LE, Artavanis-Tsakonas K, Ploegh HL, Wilson JA, Cox GA *et al.* (2008) Differential effects of Usp14 and Uch-L1 on the ubiquitin proteasome system and synaptic activity. *Mol Cell Neurosci* **39**, 539–548.
21 Miyoshi Y, Nakayama S, Torikoshi Y, Tanaka S, Ishihara H, Taguchi T, Tamaki Y & Noguchi S (2006) High expression of ubiquitin carboxy-terminal hydrolase-L1 and -L3 mRNA predicts early recurrence in patients with invasive breast cancer. *Cancer Sci* **97**, 523–529.
22 Carmine Belin A, Westerlund M, Bergman O, Nissbrandt H, Lind C, Sydow O & Galter D (2007) S18Y in ubiquitin carboxy-terminal hydrolase L1 (UCH-L1) associated with decreased risk of Parkinson's disease in Sweden. *Parkinsonism Relat Disord* **13**, 295–298.

23 Gong B, Cao ZX, Zheng P, Vitolo OV, Liu SM, Staniszewski A, Moolman D, Zhang H, Shelanski M & Arancio O (2006) Ubiquitin hydrolase Uch-L1 rescues beta-amyloid-induced decreases in synaptic function and contextual memory. *Cell* **126**, 775–788.
24 Setsuie R & Wada K (2007) The functions of UCH-L1 and its relation to neurodegenerative diseases. *Neurochem Int* **51**, 105–111.
25 Huang L & Makarov DE (2008) Translocation of a knotted polypeptide through a pore. *J Chem Phys* **129**, doi:10.1063/1.2968554.
26 Jackson SE & Fersht AR (1991) Folding of chymotrypsin inhibitor-2.1. Evidence for a 2-state transition. *Biochemistry* **30**, 10428–10435.
27 Wallace LA & Matthews CR (2002) Sequential vs. parallel protein-folding mechanisms: experimental tests for complex folding reactions. *Biophys Chem* **101**, 113–131.
28 Grathwohl C & Wuthrich K (1981) NMR-studies of the rates of proline *cis–trans* isomerization in oligopeptides. *Biopolymers* **20**, 2623–2633.
29 Ruan K & Balny C (2002) High pressure static fluorescence to study macromolecular structure–function. *Biochim Biophys Acta Protein Struct Mol Enzymol* **1595**, 94–102.
30 Ervin J, Larios E, Osvath S, Schulten K & Gruebele M (2002) What causes hyperfluorescence: folding intermediates or conformationally flexible native states? *Biophys J* **83**, 473–483.
31 Ayed A & Duckworth H (1999) A stable intermediate in the equilibrium unfolding of *Escherichia coli* citrate synthase. *Protein Sci* **8**, 1116–1126.
32 Jemth P, Gianni S, Day R, Li B, Johnson CM, Daggett V & Fersht AR (2004) Demonstration of a low-energy on-pathway intermediate in a fast-folding protein by kinetics, protein engineering, and simulation. *Proc Natl Acad Sci USA* **101**, 6450–6455.
33 Pradeep L, Shin H-C & Scheraga HA (2006) Correlation of folding kinetics with the number and isomerization states of prolines in three homologous proteins of the RNase family. *FEBS Lett* **580**, 5029–5032.
34 Capaldi AP, Shastry MCR, Kleanthous C, Roder H & Radford SE (2001) Ultrarapid mixing experiments reveal that Im7 folds via an on-pathway intermediate. *Nat Struct Mol Biol* **8**, 68–72.
35 Eifler N, Vetsch M, Gregorini M, Ringler P, Chami M, Philippsen A, Fritz A, Muller SA, Glockshuber R, Engel A *et al.* (2006) Cytotoxin ClyA from *Escherichia coli* assembles to a 13-meric pore independent of its redox-state. *EMBO J* **25**, 2652–2661.
36 Friel CT, Beddard GS & Radford SE (2004) Switching two-state to three-state kinetics in the helical protein Im9 via the optimisation of stabilising non-native interactions by design. *J Mol Biol* **342**, 261–273.
37 Otto MR, Lillo MP & Beechem JM (1994) Resolution of multiphasic reactions by the combination of fluorescence total-intensity and anistropy stopped-flow kinetic-experiments. *Biophys J* **67**, 2511–2521.
38 Chen Y & Barkley MD (1998) Toward understanding tryptophan fluorescence in proteins. *Biochemistry* **37**, 9976–9982.
39 Roder H, Maki K & Cheng H (2006) Early events in protein folding explored by rapid mixing methods. *Chem Rev* **106**, 1836–1861.
40 Royer CA, Mann CJ & Matthews CR (1993) Resolution of the fluorescence equilibrium unfolding profile of Trp apo-repressor using single tryptophan mutants. *Protein Sci* **2**, 1844–1852.

Supporting information

The following supplementary material is available:
Fig. S1. Hydrophobic residues in close proximity to Trp29.

This supplementary material can be found in the online version of this article.

Please note: Wiley-Blackwell is not responsible for the content or functionality of any supplementary materials supplied by the authors. Any queries (other than missing material) should be directed to the corresponding author for the article.